Exact Solution for Simply Supported and Multilayered Magneto-Electro-Elastic Plates

E. Pan
Structures Technology, Inc.
543 Keisler Drive, Suite 204,
Cary, NC 27511
e-mail: pan@ipass.net

Exact solutions are derived for three-dimensional, anisotropic, linearly magneto-electro-elastic, simply-supported, and multilayered rectangular plates under static loadings. While the homogeneous solutions are obtained in terms of a new and simple formalism that resemble the Stroh formalism, solutions for multilayered plates are expressed in terms of the propagator matrix. The present solutions include all the previous solutions, such as piezoelectric, piezomagnetic, purely elastic solutions, as special cases, and can therefore serve as benchmarks to check various thick plate theories and numerical methods used for the modeling of layered composite structures. Typical numerical examples are presented and discussed for layered piezoelectric/piezomagnetic plates under surface and internal loads. [DOI: 10.1115/1.1380385]

Introduction

Because of their analytical nature, exact solutions for simply-supported (layered) plates under static loadings are still of particular values. These solutions can predict exactly the behaviors of elastic deformations and stresses near or across the interface of material layers, and can thus be used to check the accuracy of various numerical methods for more complicated applications ([1]). For anisotropic elastic composites, Pagano [2,3], Srinivas et al. [4], and Srinivas and Rao [5] derived the classic solutions for both the cylindrical and rectangular plates. While the author ([6]) introduced the propagator matrix method ([7]) to handle the corresponding multilayered case, Noor and Burton [8] derived analytical solutions for laminated anisotropic plates.

Recent development of piezoelectric ceramics has stimulated considerable studies on the electric and mechanical behaviors of piezoelectric structures. Again, analytical solutions, even though under certain assumptions, are still desirable. Extensions of the elastostatic solutions for simply-supported plates to the corresponding piezoelectric cases were carried out by Ray and co-workers [9,10], Heyliger and co-workers [11,12], Bisegna and Maceri [13], and Lee and Jiang [14]. Very recently, Vel and Batra [15] presented an analytical solution for multilayered piezoelectric plates in terms of the double Fourier series to handle more general boundary conditions at the edges.

More recent advances are the smart or intelligent materials where piezoelectric and piezomagnetic materials are involved. These materials have the ability of converting energy from one form (among magnetic, electric, and mechanical energies) to the other ([16–18]). Furthermore, composites made of piezoelectric/piezomagnetic materials exhibit magnetoelectric effect that is not present in single-phase piezoelectric or piezomagnetic materials ([19–21]). Although various inclusion-related problems in these materials have been investigated in recent years ([20–24]), no three-dimensional solution is available for the simply supported plate made of piezoelectric/piezomagnetic materials.

In this paper, we derive the exact solutions for three-dimensional, anisotropic magneto-electro-elastic, simply-supported, and multilayered rectangular plates under both surface and internal loads. The general solution in a homogeneous plate is obtained in terms of a new and simple formalism that resembles the Stroh formalism ([25–27]). In order to treat a multilayered plate, the propagator matrix method is introduced with which the corresponding multilayered solution has an elegant and simple expression. To the best of the author's knowledge, it is the first time that a piezoelectric and magnetostrictive multilayered plate under simple supporting conditions is analytically studied. It is also the first time that an internal loading case is investigated and compared to the surface loading case. The present solutions include all the previous solutions, such as the piezoelectric, piezomagnetic, purely elastic solutions, as special cases. Since the present solutions are exact, they can serve as benchmarks to test various thick plate theories and various numerical methods, such as the finite and boundary element methods, used for the modeling of layered composite structures.

As a numerical illustration, a piezoelectric and homogeneous plate under surface and internal loads and a sandwich plate made of piezoelectric $BaTiO_3$ and magnetostrictive $CoFe_2O_4$ under a surface mechanical load are analyzed. It is very interesting that even for a relatively thin plate, responses from an internal load are quite different to those from a surface load. For the sandwich plate made of piezoelectric $BaTiO_3$ and magnetostrictive $CoFe_2O_4$, it is observed that responses from different stacking sequences are completely different, especially for the electric and magnetic quantities. These new numerical results should be of special interest to the design of magneto-electro-elastic composite laminates.

Problem Description and Basic Equations

Let us consider an anisotropic, magneto-electro-elastic, and N-layered rectangular plate with horizontal dimensions L_x and L_y and total thickness H (in the vertical direction) with its four sides being simply supported. A Cartesian coordinate system $(x,y,z) = (x_1,x_2,x_3)$ is attached to the plate in such a way that its origin is at one of the four corners on the bottom surface and the plate is in the positive z region. Let layer j be bonded by the lower interface z_j and the upper interface z_{j+1} with thickness $h_j = z_{j+1} - z_j$. It is obvious that $z_1 = 0$ and $z_{N+1} = H$. Material properties in each layer can be different, and internal and/or surface loads (mechanical, electric or magnetic) can be applied. Along the interface, the extended displacement and traction vectors (to be defined later) are assumed to be continuous, with the exception of the internal loading level, which will be discussed later. Without loss of generality, we also assume that the surface load is applied on the top surface of the layered plate.

Contributed by the Applied Mechanics Division of THE AMERICAN SOCIETY OF MECHANICAL ENGINEERS for publication in the ASME JOURNAL OF APPLIED MECHANICS. Manuscript received by the ASME Applied Mechanics Division, April 2, 2000; final revision, January 30, 2001. Associate Editor: W. J. Drugan. Discussion on the paper should be addressed to the Editor, Prof. Lewis T. Wheeler, Department of Mechanical Engineering, University of Houston, Houston, TX 77204-4792, and will be accepted until four months after final publication of the paper itself in the ASME JOURNAL OF APPLIED MECHANICS.

For an anisotropic and linearly magneto-electro-elastic solid, the coupled constitutive relation can be written as ([16])

$$\sigma_i = C_{ik}\gamma_k - e_{ki}E_k - q_{ki}H_k$$
$$D_i = e_{ik}\gamma_k + \varepsilon_{ik}E_k + d_{ik}H_k$$
$$B_i = q_{ik}\gamma_k + d_{ik}E_k + \mu_{ik}H_k \tag{1}$$

where σ_i, D_i, and B_i are the stress, electric displacement, and magnetic induction (i.e., magnetic flux), respectively; γ_i, E_i, and H_i are the strain, electric field, and magnetic field, respectively; C_{ij}, ε_{ij}, and μ_{ij} are the elastic, dielectric, and magnetic permeability coefficients, respectively; e_{ij}, q_{ij}, and d_{ij} are the piezoelectric, piezomagnetic, and magnetoelectric coefficients, respectively. It is obvious that various uncoupled cases can be reduced from Eq. (1) by setting the appropriate coefficients to zero.

For an orthotropic solid, with transverse isotropy being a special case, the material constant matrices of Eq. (1) are expressed by

$$[C] = \begin{bmatrix} C_{11} & C_{12} & C_{13} & 0 & 0 & 0 \\ & C_{22} & C_{23} & 0 & 0 & 0 \\ & & C_{33} & 0 & 0 & 0 \\ & & & C_{44} & 0 & 0 \\ & \text{Sym} & & & C_{55} & 0 \\ & & & & & C_{66} \end{bmatrix},$$

$$[e] = \begin{bmatrix} 0 & 0 & e_{31} \\ 0 & 0 & e_{32} \\ 0 & 0 & e_{33} \\ 0 & e_{24} & 0 \\ e_{15} & 0 & 0 \\ 0 & 0 & 0 \end{bmatrix}, \quad [q] = \begin{bmatrix} 0 & 0 & q_{31} \\ 0 & 0 & q_{32} \\ 0 & 0 & q_{33} \\ 0 & q_{24} & 0 \\ q_{15} & 0 & 0 \\ 0 & 0 & 0 \end{bmatrix} \tag{2}$$

$$[\varepsilon] = \begin{bmatrix} \varepsilon_{11} & 0 & 0 \\ 0 & \varepsilon_{22} & 0 \\ 0 & 0 & \varepsilon_{33} \end{bmatrix}, \quad [d] = \begin{bmatrix} d_{11} & 0 & 0 \\ 0 & d_{22} & 0 \\ 0 & 0 & d_{33} \end{bmatrix},$$

$$[\mu] = \begin{bmatrix} \mu_{11} & 0 & 0 \\ 0 & \mu_{22} & 0 \\ 0 & 0 & \mu_{33} \end{bmatrix}. \tag{3}$$

The extended strain (using tensor symbol for the elastic strain γ_{ik})-displacement relation is

$$\gamma_{ij} = 0.5(u_{i,j} + u_{j,i})$$
$$E_i = -\phi_{,i}, \quad H_i = -\psi_{,i} \tag{4}$$

where u_i, ϕ, and ψ are the elastic displacement, electric potential, and magnetic potential, respectively.

The equations of equilibrium, including the balance of the body force and electric charge and current, can be written as

$$\sigma_{ij,j} + f_i = 0$$
$$D_{j,j} - f_e = 0$$
$$B_{j,j} - f_m = 0 \tag{5}$$

where f_i, f_e, and f_m are the body force, electric charge density, and electric current density, respectively. The electric current density is also called magnetic charge density as compared to the electric charge density.

General Solutions

For a simply-supported and homogeneous plate, we seek the solution of the extended displacement vector in the form of

$$\mathbf{u} \equiv \begin{bmatrix} u_1 \\ u_2 \\ u_3 \\ \phi \\ \psi \end{bmatrix} = e^{sz} \begin{bmatrix} a_1 \cos px \sin qy \\ a_2 \sin px \cos qy \\ a_3 \sin px \sin qy \\ a_4 \sin px \sin qy \\ a_5 \sin px \sin qy \end{bmatrix} \tag{6}$$

where

$$p = n\pi/L_x, \quad q = m\pi/L_y \tag{7}$$

and n and m are two positive integers.

It is noted that solution (6) represents only one of the terms in a double Fourier series expansion when solving a general boundary value problem. Therefore, in general, summations for n and m over suitable ranges are implied whenever the sinusoidal term appears.

Substitution of Eq. (6) into the strain-displacement relation (4) and subsequently into the constitutive relation (1) yields the extended traction vector

$$\mathbf{t} \equiv \begin{bmatrix} \sigma_{13} \\ \sigma_{23} \\ \sigma_{33} \\ D_3 \\ B_3 \end{bmatrix} = e^{sz} \begin{bmatrix} b_1 \cos px \sin qy \\ b_2 \sin px \cos qy \\ b_3 \sin px \sin qy \\ b_4 \sin px \sin qy \\ b_5 \sin px \sin qy \end{bmatrix}. \tag{8}$$

Introducing two vectors

$$\mathbf{a} = [a_1, a_2, a_3, a_4, a_5]^t, \quad \mathbf{b} = [b_1, b_2, b_3, b_4, b_5]^t \tag{9}$$

we then find that the vector $\mathbf{b}$ is related to $\mathbf{a}$ by

$$\mathbf{b} = (-\mathbf{R}^t + s\mathbf{T})\mathbf{a} = -\frac{1}{s}(\mathbf{Q} + s\mathbf{R})\mathbf{a} \tag{10}$$

where the superscript t denotes matrix transpose, and

$$\mathbf{R} = \begin{bmatrix} 0 & 0 & pC_{13} & pe_{31} & pq_{31} \\ 0 & 0 & qC_{23} & qe_{32} & pq_{32} \\ -pC_{55} & -qC_{44} & 0 & 0 & 0 \\ -pe_{15} & -qe_{24} & 0 & 0 & 0 \\ -pq_{15} & -qq_{24} & 0 & 0 & 0 \end{bmatrix},$$

$$\mathbf{T} = \begin{bmatrix} C_{55} & 0 & 0 & 0 & 0 \\ & C_{44} & 0 & 0 & 0 \\ & & C_{33} & e_{33} & q_{33} \\ & & & -\varepsilon_{33} & -d_{33} \\ & & & & -\mu_{33} \end{bmatrix} \tag{11}$$

$$
\mathbf{Q}=\begin{bmatrix} -(C_{11}p^2+C_{66}q^2) & -pq(C_{12}+C_{66}) & 0 & 0 & 0 \\ & -(C_{66}p^2+C_{22}q^2) & 0 & 0 & 0 \\ & & -(C_{55}p^2+C_{44}q^2) & -(e_{15}p^2+e_{24}q^2) & -(q_{15}p^2+q_{24}q^2) \\ & & & \varepsilon_{11}p^2+\varepsilon_{22}q^2 & d_{11}p^2+d_{22}q^2 \\ & & & & \mu_{11}p^2+\mu_{22}q^2 \end{bmatrix}. \tag{12}
$$

We mention that matrices $\mathbf{Q}$ and $\mathbf{T}$ are symmetric.

The in-plane stresses and electric and magnetic displacements are obtained as

$$
\begin{bmatrix} \sigma_{11} \\ \sigma_{12} \\ \sigma_{22} \\ D_1 \\ D_2 \\ B_1 \\ B_2 \end{bmatrix} = e^{sz} \begin{bmatrix} c_1 \sin px \sin qy \\ c_2 \cos px \cos qy \\ c_3 \sin px \cos qy \\ c_4 \cos px \sin qy \\ c_5 \sin px \cos qy \\ c_6 \cos px \sin qy \\ c_7 \sin px \cos qy \end{bmatrix} \tag{13}
$$

where

$$
\begin{bmatrix} c_1 \\ c_2 \\ c_3 \\ c_4 \\ c_5 \\ c_6 \\ c_7 \end{bmatrix} = \begin{bmatrix} -C_{11}p & -C_{12}q & C_{13}s & e_{31}s & q_{31}s \\ C_{66}q & C_{66}p & 0 & 0 & 0 \\ -C_{12}p & -C_{22}q & C_{23}s & e_{32}s & q_{32}s \\ e_{15}s & 0 & e_{15}p & -\varepsilon_{11}p & -d_{11}p \\ 0 & e_{24}s & e_{24}q & -\varepsilon_{22}q & -d_{22}q \\ q_{15}s & 0 & q_{15}p & -d_{11}p & -\mu_{11}p \\ 0 & q_{24}s & q_{24}q & -d_{22}q & -\mu_{22}q \end{bmatrix} \begin{bmatrix} a_1 \\ a_2 \\ a_3 \\ a_4 \\ a_5 \end{bmatrix}. \tag{14}
$$

These extended stresses (Eqs. (8) and (13)) should satisfy the equations of equilibrium (assuming zero body force and zero electric and magnetic charge densities), which in terms of the vector $\mathbf{a}$, yields the following eigenequation:

$$
[\mathbf{Q}+s(\mathbf{R}+\mathbf{R}')+s^2\mathbf{T}]\mathbf{a}=0 \tag{15}
$$

where $\mathbf{R}'=-\mathbf{R}^t$.

It is noted that Eq. (15), derived for a simply supported plate, resembles the Stroh formalism ([25,26]). However, their solution structures are different because of the slightly different features of the $\mathbf{R}$ matrix (in the Stroh formalism, $\mathbf{R}'=\mathbf{R}^t$). It is known that in the Stroh formalism, positive internal energy requirement guarantees that the characteristic roots of Eq. (15) should be complex numbers with nonvanishing imaginary parts; they cannot be real ([26]). In the present formalism, however, such a feature does not exist. Instead, since a matrix and its transpose have the same determinant value, we conclude that if s is an eigenvalue of Eq. (15), so is $-s$. Furthermore, if s is a complex (or purely imaginary) eigenvalue, then its complex conjugate is also an eigenvalue since all the coefficient matrices in Eq. (15) are real. We name Eq. (15) as the pseudo-Stroh formalism because of its similarity to the Stroh formalism.

With aid of Eq. (10), Eq. (15) can now be recast into a 10×10 linear eigensystem

$$
\mathbf{N}\begin{bmatrix} \mathbf{a} \\ \mathbf{b} \end{bmatrix} = s\begin{bmatrix} \mathbf{a} \\ \mathbf{b} \end{bmatrix} \tag{16}
$$

where

$$
\mathbf{N}=\begin{bmatrix} -\mathbf{T}^{-1}\mathbf{R}' & \mathbf{T}^{-1} \\ -\mathbf{Q}+\mathbf{R}\mathbf{T}^{-1}\mathbf{R}' & -\mathbf{R}\mathbf{T}^{-1} \end{bmatrix}. \tag{17}
$$

Depending upon the given material property, the ten eigenvalues of Eq. (16) may not be distinct. Should repeated roots occur, a slight change in the material constants would result in distinct roots with negligible error ([28]) so that the following simple solution structure can still be applied.

Therefore, let us assume that the first five eigenvalues have positive real parts (if the root is purely imaginary, we then pick up the one with positive imaginary part) and the remainder have opposite signs to the first five. We distinguish the corresponding ten eigenvectors by attaching a subscript to $\mathbf{a}$ and $\mathbf{b}$. Then the general solution for the extended displacement and traction vectors (of the z-dependent factor) are derived as

$$
\begin{bmatrix} \mathbf{u} \\ \mathbf{t} \end{bmatrix} = \begin{bmatrix} \mathbf{A}_1 & \mathbf{A}_2 \\ \mathbf{B}_1 & \mathbf{B}_2 \end{bmatrix} \langle e^{s^*z} \rangle \begin{bmatrix} \mathbf{K}_1 \\ \mathbf{K}_2 \end{bmatrix} \tag{18}
$$

where

$$
\mathbf{A}_1=[\mathbf{a}_1,\mathbf{a}_2,\mathbf{a}_3,\mathbf{a}_4,\mathbf{a}_5], \quad \mathbf{A}_2=[\mathbf{a}_6,\mathbf{a}_7,\mathbf{a}_8,\mathbf{a}_9,\mathbf{a}_{10}]
$$

$$
\mathbf{B}_1=[\mathbf{b}_1,\mathbf{b}_2,\mathbf{b}_3,\mathbf{b}_4,\mathbf{b}_5], \quad \mathbf{B}_2=[\mathbf{b}_6,\mathbf{b}_7,\mathbf{b}_8,\mathbf{b}_9,\mathbf{b}_{10}]
$$

$$
\langle e^{s^*z} \rangle = \mathrm{diag}[e^{s_1z},e^{s_2z},e^{s_3z},e^{s_4z},e^{s_5z},e^{-s_1z},e^{-s_2z},e^{-s_3z},e^{-s_4z},e^{-s_5z}]
$$

and $\mathbf{K}_1$ and $\mathbf{K}_2$ are two 5×1 constant column matrices to be determined.

Equation (18) is a general solution for a homogeneous, magneto-electro-elastic, and simply-supported plate, and contains previous piezoelectric and purely elastic solutions as its special cases. Clearly, in spite of the complicated nature of the problem, the general solution is remarkably simple. Furthermore, certain thin plate results can also be reduced from this solution by expanding the exponential term in terms of a Taylor series ([29,30]). This is particularly easy since one needs only to replace the diagonal exponential matrix with its Taylor series expansion ([6,13]). We mention that although other methods, such as the state space approach ([14]), may also be employed to derive a general solution for such a plate, more algebraic manipulations are needed. Furthermore, reduction to the thin plate result is complicated if a state space approach is followed.

With Eq. (18) being served as a general solution for a homogeneous and magneto-electro-elastic plate, solutions for the corresponding multilayered plate can be obtained using the continuity conditions along the interface and the boundary conditions on the top and bottom surfaces of the plate. In doing so, a system of linear equations for the unknowns can be formed and solved ([3,12]). However, for structures with relatively large numbers of layers (say, up to a hundred layers), the system of linear equations then becomes very large, and the propagator matrix method developed exclusively for layered structures can be conveniently and efficiently applied (for a brief review, see [31]). We discuss this matter in the next section.

Propagator Matrix and Solution of Layered System

Since the matrix $\mathbf{N}$, defined in Eq. (17), is not symmetric, the eigenvectors of Eq. (16) are actually the right ones. The left eigenvectors are found by solving the following eigenvalue system:

$$
\mathbf{N}^t \boldsymbol{\eta} = \lambda \boldsymbol{\eta}. \tag{19}
$$

It is a matter of simple fact that if s and $[\mathbf{a},\mathbf{b}]^t$ are the eigenvalue and eigenvector of Eq. (16), then $\lambda=-s$ and $\eta=[-\mathbf{b},\mathbf{a}]^t$ are the corresponding solutions of Eq. (19). Since the left and right eigenvectors are orthogonal to each other, we then come to the following important relation:

$$\begin{bmatrix} -\mathbf{B}_2^t & \mathbf{A}_2^t \\ \mathbf{B}_1^t & -\mathbf{A}_1^t \end{bmatrix}\begin{bmatrix} \mathbf{A}_1 & \mathbf{A}_2 \\ \mathbf{B}_1 & \mathbf{B}_2 \end{bmatrix}=\begin{bmatrix} \mathbf{I} & \mathbf{0} \\ \mathbf{0} & \mathbf{I} \end{bmatrix} \tag{20}$$

where $\mathbf{I}$ is a 5×5 unit matrix, and the eigenvectors have been normalized according to

$$-\mathbf{B}_2^t\mathbf{A}_1+\mathbf{A}_2^t\mathbf{B}_1=\mathbf{I} \tag{21}$$

Equation (20) resembles the orthogonal relation in the Stroh formalism ([26]) and provides us with a simple way of inverting the eigenvector matrix, which is required in forming the propagator matrix.

Let us assume that Eq. (18) is a general solution in the homogeneous layer j, with the top and bottom boundaries locally at h and 0, respectively. Let $z=0$ in Eq. (18) and solve for the unknown constant column matrix, we find that

$$\begin{bmatrix} \mathbf{K}_1 \\ \mathbf{K}_2 \end{bmatrix}=\begin{bmatrix} \mathbf{A}_1 & \mathbf{A}_2 \\ \mathbf{B}_1 & \mathbf{B}_2 \end{bmatrix}^{-1}\begin{bmatrix} \mathbf{u} \\ \mathbf{t} \end{bmatrix}_0=\begin{bmatrix} -\mathbf{B}_2^t & \mathbf{A}_2^t \\ \mathbf{B}_1^t & -\mathbf{A}_1^t \end{bmatrix}\begin{bmatrix} \mathbf{u} \\ \mathbf{t} \end{bmatrix}_0. \tag{22}$$

The second equation follows from Eq. (20). Therefore, the solution in the homogeneous layer j at any level z can be expressed by that at $z=0$ as

$$\begin{bmatrix} \mathbf{u} \\ \mathbf{t} \end{bmatrix}_z=\mathbf{P}(z)\begin{bmatrix} \mathbf{u} \\ \mathbf{t} \end{bmatrix}_0 \tag{23}$$

where

$$\mathbf{P}(z)=\begin{bmatrix} \mathbf{A}_1 & \mathbf{A}_2 \\ \mathbf{B}_1 & \mathbf{B}_2 \end{bmatrix}\langle e^{s^*z}\rangle\begin{bmatrix} -\mathbf{B}_2^t & \mathbf{A}_2^t \\ \mathbf{B}_1^t & -\mathbf{A}_1^t \end{bmatrix} \tag{24}$$

is called the propagator matrix ([7,31]). Listed below are three important features of the propagator matrix, which can be proved easily.

$$\mathbf{P}(0)=\begin{bmatrix} \mathbf{I} & \mathbf{0} \\ \mathbf{0} & \mathbf{I} \end{bmatrix} \tag{25}$$

$$\mathbf{P}(z_3-z_1)=\mathbf{P}(z_3-z_2)\mathbf{P}(z_2-z_1) \tag{26}$$

$$\mathbf{P}(z_3-z_1)=\mathbf{P}^{-1}(z_1-z_3) \tag{27}$$

The propagating relation (23) can be used repeatedly so that one can propagate the physical quantities from the bottom surface $z=0$ to the top surface $z=H$ of the layered plate. Consequently, we have

$$\begin{bmatrix} \mathbf{u} \\ \mathbf{t} \end{bmatrix}_H=\mathbf{P}_N(h_N)\mathbf{P}_{N-1}(h_{N-1})\ \ldots\ \ldots\ \mathbf{P}_2(h_2)\mathbf{P}_1(h_1)\begin{bmatrix} \mathbf{u} \\ \mathbf{t} \end{bmatrix}_0 \tag{28}$$

where $h_j=z_{j+1}-z_j$ is the thickness of layer j and $\mathbf{P}_j$ the propagator matrix of the same layer.

Equation (28) is a surprisingly simple relation and, for given boundary conditions, can be solved for the unknowns involved. As an example, we assume that, on the top surface ($z=H$) the z-direction traction component is applied, i.e.,

$$\sigma_{zz}=\sigma_0 \sin px \sin qy \tag{29}$$

which may represent one of the terms in the double Fourier series solution for a general loading case (uniform or point loading), and all other traction components on both surfaces are zero (i.e., the second-type boundary value problem). Equation (28) is then reduced to

$$\begin{bmatrix} \mathbf{u}(H) \\ \mathbf{t}(H) \end{bmatrix}=\begin{bmatrix} \mathbf{C}_1 & \mathbf{C}_2 \\ \mathbf{C}_3 & \mathbf{C}_4 \end{bmatrix}\begin{bmatrix} \mathbf{u}(0) \\ \mathbf{0} \end{bmatrix} \tag{30}$$

where the four submatrices $\mathbf{C}_j$ are the multiplications of the propagator matrices in Eq. (28), and $\mathbf{t}(H)$ is the given boundary condition on the top surface, i.e.,

$$t(H)=[0,0,\sigma_0 \sin px \sin qy,0,0]^t. \tag{31}$$

Solving the unknown extended displacements on both surfaces of the layered plate, we find

$$\mathbf{u}(0)=\mathbf{C}_3^{-1}\mathbf{t}(H)$$

$$\mathbf{u}(H)=\mathbf{C}_1\mathbf{C}_3^{-1}\mathbf{t}(H). \tag{32}$$

In order to obtain the extended displacement and traction vectors at any depth, say $z_k\leqslant z\leqslant z_{k+1}$ in layer k, we propagate the solution from the bottom of the surface to the z-level ([31]), i.e.,

$$\begin{bmatrix} \mathbf{u} \\ \mathbf{t} \end{bmatrix}_z=\mathbf{P}_k(z-z_{k-1})\mathbf{P}_{k-1}(h_{k-1})\ \ldots\ \ldots\ \mathbf{P}_2(h_2)\mathbf{P}_1(h_1)\begin{bmatrix} \mathbf{u} \\ \mathbf{t} \end{bmatrix}_0. \tag{33}$$

With the extended displacement and traction vectors at a given depth being solved, the corresponding in-plane quantities can be evaluated using Eqs. (13) and (14).

Similar solutions can also be obtained for the first-type boundary value problem (i.e., for given extended displacement vectors on both surfaces) and for the third-type, i.e., the mixed boundary value problem as well. Therefore, for an anisotropic, magneto-electro-elastic, and simply-supported multilayered rectangular plate, we have derived the exact solution based on the pseudo-Stroh formalism and the propagator matrix method.

The present methodology can also be equally and easily extended to the corresponding internal loading case, which is of significance to the Green's function study. We now seek such a solution.

If there is an internal source (force, charge, dislocation, etc.) located at $z=d_0$ level within layer $j(z_{j+1},z_j)$, we artificially divide this layer into two sublayers $j1(d_0,z_j)$ (with $h_{j1}=d_0-z_j$) and $j2(z_{j+1},d_0)$ (with $h_{j2}=z_{j+1}-d_0$), and define the discontinuities across the source level as

$$\begin{bmatrix} \Delta\mathbf{u} \\ \Delta\mathbf{t} \end{bmatrix}\equiv\begin{bmatrix} \mathbf{u}(d_0+0) \\ \mathbf{t}(d_0+0) \end{bmatrix}-\begin{bmatrix} \mathbf{u}(d_0-0) \\ \mathbf{t}(d_0-0) \end{bmatrix}. \tag{34}$$

Again, propagating the propagator matrices from the bottom to the top of the surfaces and making use of the discontinuity relation (34) ([31,32]), we arrive at the following important equation:

$$\begin{bmatrix} \mathbf{u} \\ \mathbf{t} \end{bmatrix}_H-\mathbf{P}_N(h_N)\mathbf{P}_{N-1}(h_{N-1})\ \ldots\ \ldots\ \mathbf{P}_2(h_2)\mathbf{P}_1(h_1)\begin{bmatrix} \mathbf{u} \\ \mathbf{t} \end{bmatrix}_0$$
$$=\mathbf{P}_N(h_N)\mathbf{P}_{N-1}(h_{N-1})\ \ldots\ \ldots\ \mathbf{P}_{j+1}(h_{j+1})\mathbf{P}_{j2}(h_{j2})\begin{bmatrix} \Delta\mathbf{u} \\ \Delta\mathbf{t} \end{bmatrix}. \tag{35}$$

Clearly, this equation is more general and includes Eq. (28) as a special case (when there is no discontinuity). Similar to the surface loading case, this equation can be solved for the unknown quantities involved ([31]).

Before carrying out numerical studies using the present formulation, we remark that the present solution is valid for any integers n and m as defined by Eq. (7). In other words, the solution we have derived can be regarded as for one of the terms in a Fourier series expansion. Because of the linearity, the solution corresponding to a general loading (uniform or point loading) can be obtained by expanding the loading as a finite double Fourier series ([13,33]) and adding the responses together term by term.

Numerical Examples

Having derived the exact and simple solutions, we now present some numerical results. Before using our formalism, we first checked our solutions with some previously published results for

Table 1 Material coefficients of the piezoelectric $BaTiO_3$ (C_{ij} in $10^9\ N/m^2$, e_{ij} in C/m^2, ε_{ij} in $10^{-9}C^2/(Nm^2)$, and μ_{ij} in $10^{-6}Ns^2/C^2$)

$C_{11}=C_{22}$ 166	C_{12} 77	$C_{13}=C_{23}$ 78	C_{33} 162	$C_{44}=C_{55}$ 43	$C_{66}=0.5(C_{11}-C_{12})$ 44.5
$e_{31}=e_{32}$ −4.4	e_{33} 18.6	$e_{24}=e_{15}$ 11.6			
$\varepsilon_{11}=\varepsilon_{22}$ 11.2	ε_{33} 12.6		$\mu_{11}=\mu_{22}$ 5	μ_{33} 10	

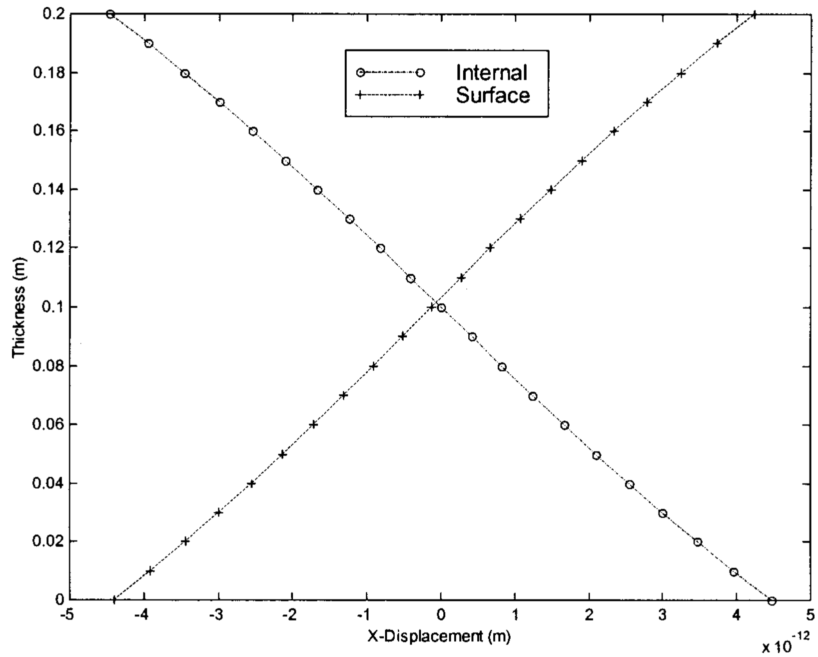

Fig. 1 Variation of the elastic displacement $u_x(=u_y)$ along the thickness direction in a homogeneous and piezoelectric plate caused by an internal load on the middle plane and a surface load on the top surface

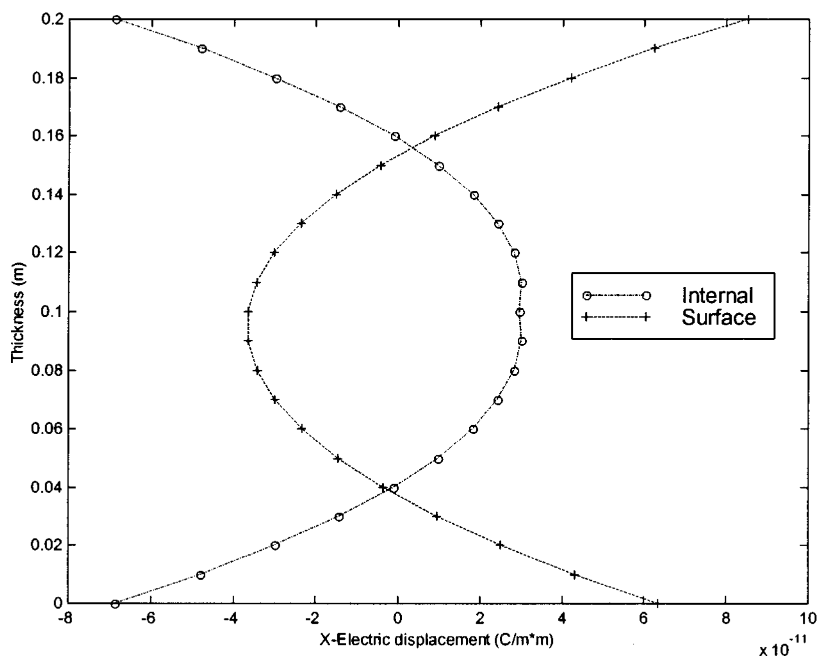

Fig. 2 Variation of the electric displacement $D_x(=D_y)$ along the thickness direction in a homogeneous and piezoelectric plate caused by an internal load on the middle plane and a surface load on the top surface

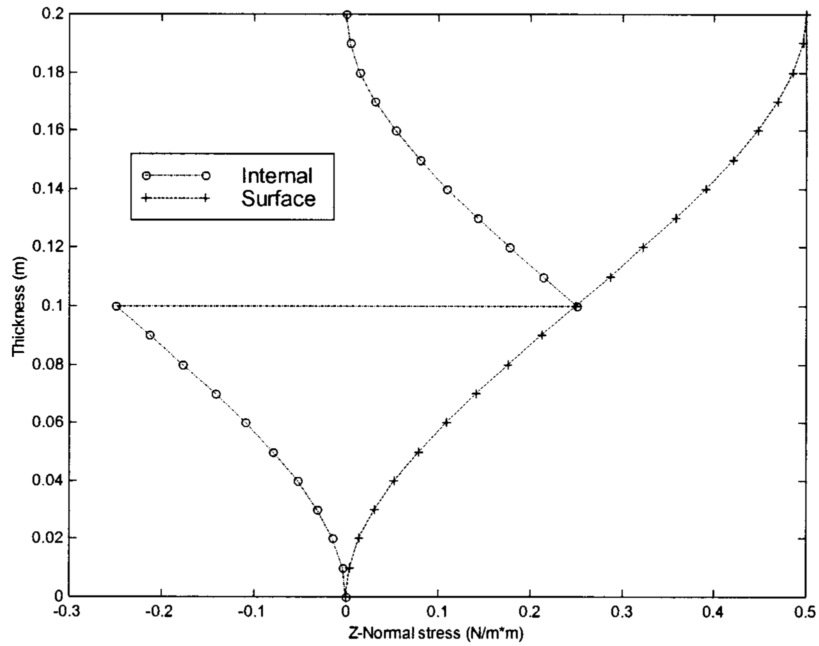

Fig. 3 Variation of the stress component σ_{zz} along the thickness direction in a homogeneous and piezoelectric plate caused by an internal load on the middle plane and a surface load on the top surface

Table 2 Material coefficients of the magnetostrictive $CoFe_2O_4$ (C_{ij} in $10^9 N/m^2$, q_{ij} in N/(Am), ε_{ij} in $10^{-9} C^2/(Nm^2)$, and μ_{ij} in $10^{-6} Ns^2/C^2$)

$C_{11}=C_{22}$	C_{12}	$C_{13}=C_{23}$	C_{33}	$C_{44}=C_{55}$	$C_{66}=0.5(C_{11}-C_{12})$
286	173	170.5	269.5	45.3	56.5
$q_{31}=q_{32}$	q_{33}	$q_{24}=q_{15}$			
580.3	699.7	550			
$\varepsilon_{11}=\varepsilon_{22}$	ε_{33}		$\mu_{11}=\mu_{22}$	μ_{33}	
0.08	0.093		−590	157	

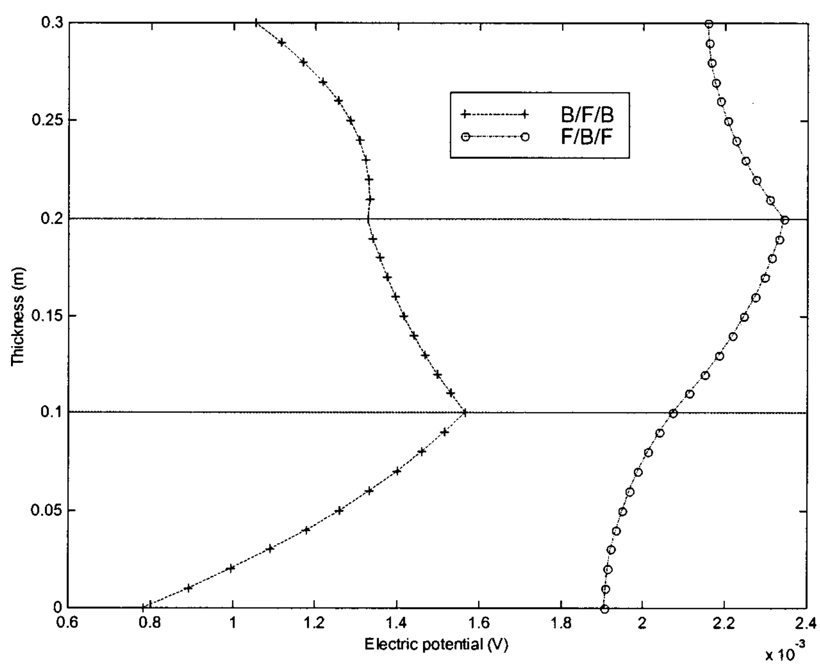

Fig. 4 Variation of the electric potential ϕ along the thickness direction in the sandwich piezoelectric/piezomagnetic plate caused by a surface load on the top surface

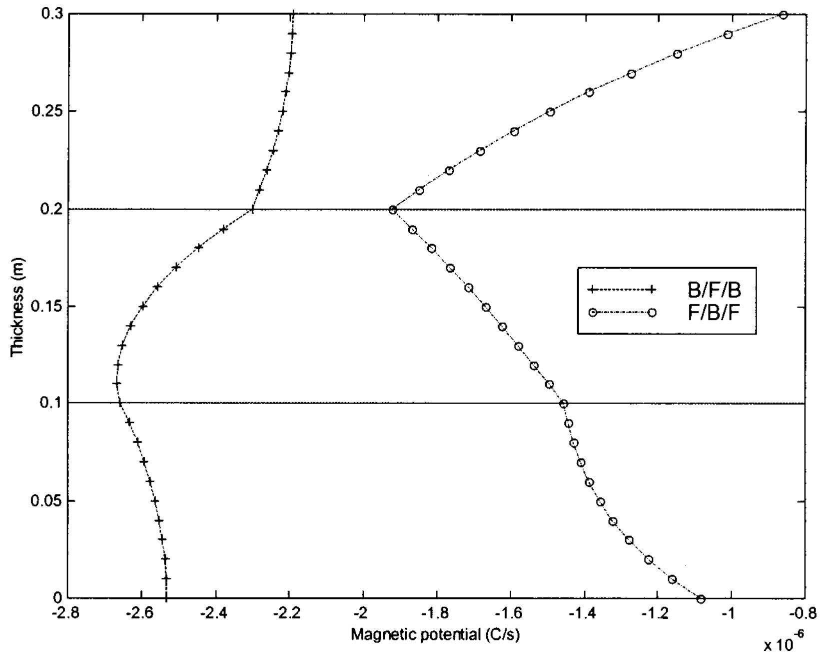

Fig. 5 Variation of the magnetic potential ψ along the thickness direction in the sandwich piezoelectric/piezomagnetic plate caused by a surface load on the top surface

both purely elastic and piezoelectric plates ([3,12,14,34]), and found that the present formulation agrees with these solutions.

The first example is for a homogeneous and transversely isotropic piezoelectric plate. The symmetry axis of the material is along the z-direction with material properties being listed in Table 1 ([14]). The dimension of the plate is $L_x \times L_y \times H = 1 \times 1 \times 0.2$ m. Two cases are studied: (1) A z-direction surface load is applied on the top surface of the plate $z = H$. That is, the extended traction is given by Eq. (31) with $m = n = 1$ (i.e., $p = \pi/L_x$, $q = \pi/L_y$) and amplitude $\sigma_0 = 1$ N/m^2. The bottom surface is assumed to be traction-free. (2) An internal load is applied on the middle plane of the plate ($z = 0.1$ m). The extended traction discontinuity $\Delta \mathbf{t}$ has a similar expression as Eq. (31) with amplitude $\Delta\sigma_{zz}$ equal to 1 N/m^2. Both the top and bottom surfaces are assumed to be traction-free. For both cases, responses are calculated for fixed horizontal coordinates $(x,y) = (0.75L_x, 0.25L_y)$.

Figures 1, 2, and 3 show the variations of the elastic displacement u_x, electric displacement D_x, and normal stress σ_{zz} along

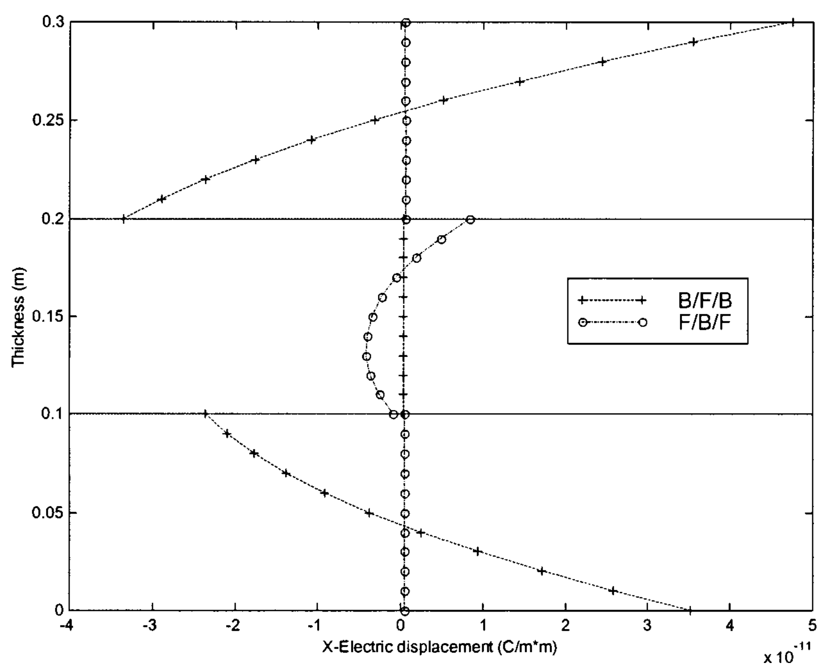

Fig. 6 Variation of the electric displacement $D_x(=D_y)$ along the thickness direction in the sandwich piezoelectric/piezomagnetic plate caused by a surface load on the top surface

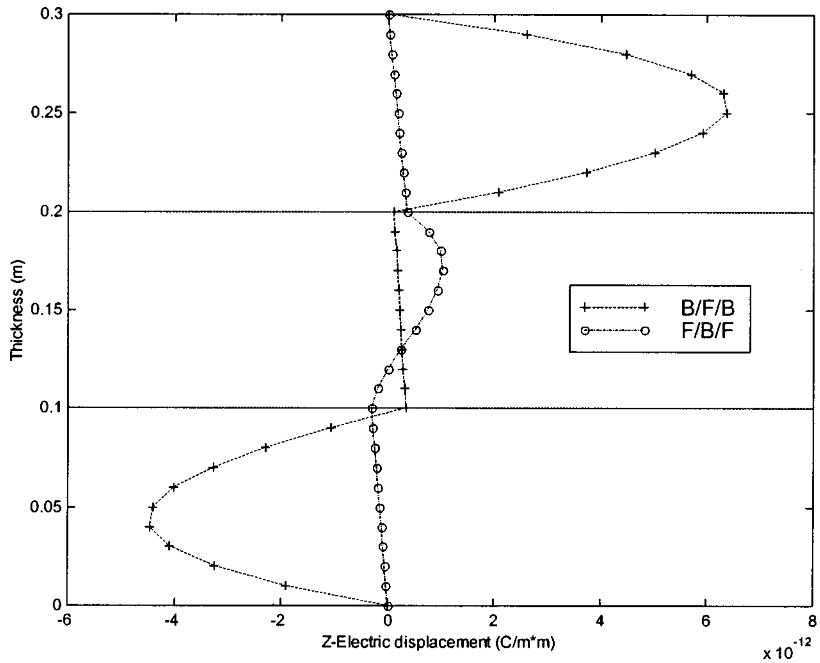

Fig. 7 Variation of the electric displacement D_z along the thickness direction in the sandwich piezoelectric/piezomagnetic plate caused by a surface load on the top surface

the thickness direction of the plate. It is clear that these two loading cases produce quite different responses in the plate, even though the plate is relative thin (with a ratio of thickness to horizontal dimension equal to 0.2). For instance, while the internal loading solution is strictly symmetric or antisymmetric with respect to the middle plane (i.e., the loading plane), the surface loading solution does not possess such features. The latter (for the elastic displacement u_x and electric displacement D_x) is only approximately symmetric or antisymmetric about the middle plane. While the normal stress σ_{zz} due to the surface load is continuous and increases monotonically from zero on the bottom surface to the applied value on the top surface, that due to the internal load is discontinuous across the loading plane $z=0.1$ m and it has opposite sign on both sides of the middle plane. The internal loading case has never been studied and compared to the surface loading case in the literature.

The second example is for sandwich plates made of piezoelectric $BaTiO_3$ and magnetostrictive $CoFe_2O_4$. The three layers have

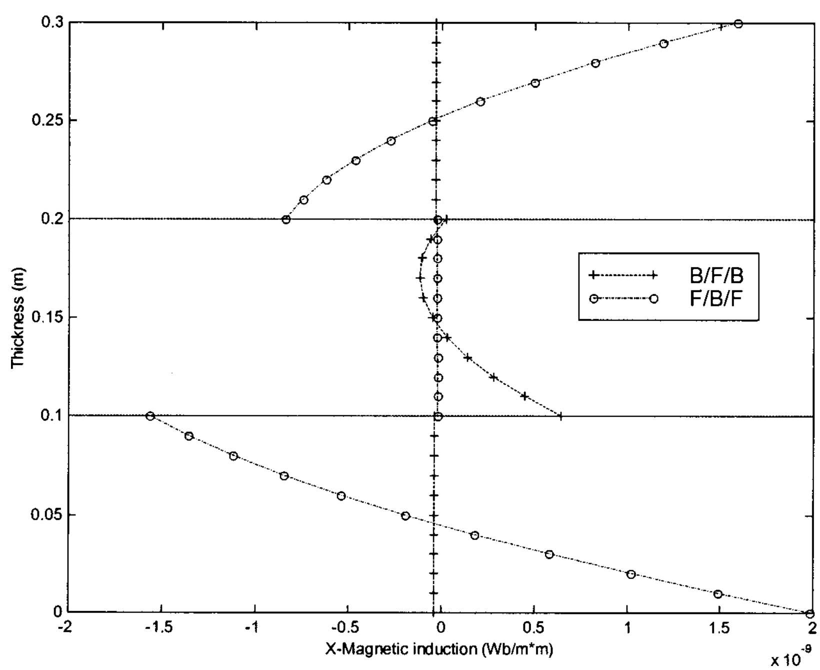

Fig. 8 Variation of the magnetic induction $B_x(=B_y)$ along the thickness direction in the sandwich piezoelectric/piezomagnetic plate caused by a surface load on the top surface

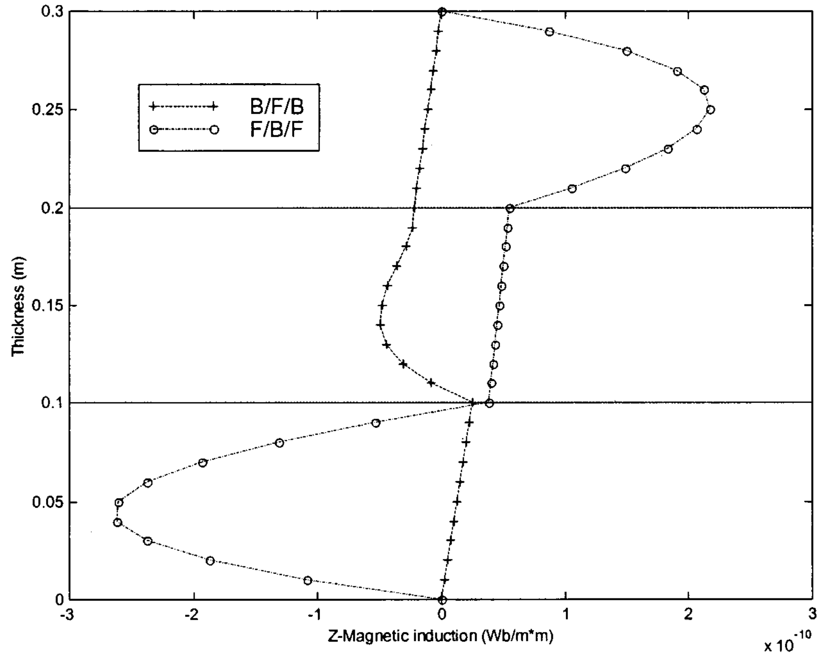

Fig. 9 Variation of the magnetic induction B_z along the thickness direction in the sandwich piezoelectric/piezomagnetic plate caused by a surface load on the top surface

equal thickness of 0.1 m (with a total thickness $H=0.3$ m). While the material properties for the piezoelectric $BaTiO_3$ are those listed in Table 1, the properties for the magnetostrictive $CoFe_2O_4$ are given in Table 2 ([35]). Similar to the piezoelectric $BaTiO_3$, the magnetostrictive $CoFe_2O_4$ is also a transversely isotropic solid with its symmetry axis along the z-axis.

Two sandwich plates with stacking sequences $BaTiO_3/CoFe_2O_4/BaTiO_3$ (called B/F/B) and $CoFe_2O_4/BaTiO_3/CoFe_2O_4$ (called F/B/F) are investigated. The surface loading as for the first example is assumed here (that is, a z-direction traction with amplitude $\sigma_0=1$ N/m^2 is applied on the top surface $z=0.3$ m while all other components on both surfaces are zero). Again, responses are calculated for fixed horizontal coordinates $(x,y)=(0.75L_x, 0.25L_y)$.

Figures 4 and 5 show, respectively, the variations of the electric and magnetic potentials along the thickness direction in the sandwich plate. It is obvious that the potential variations for the B/F/B

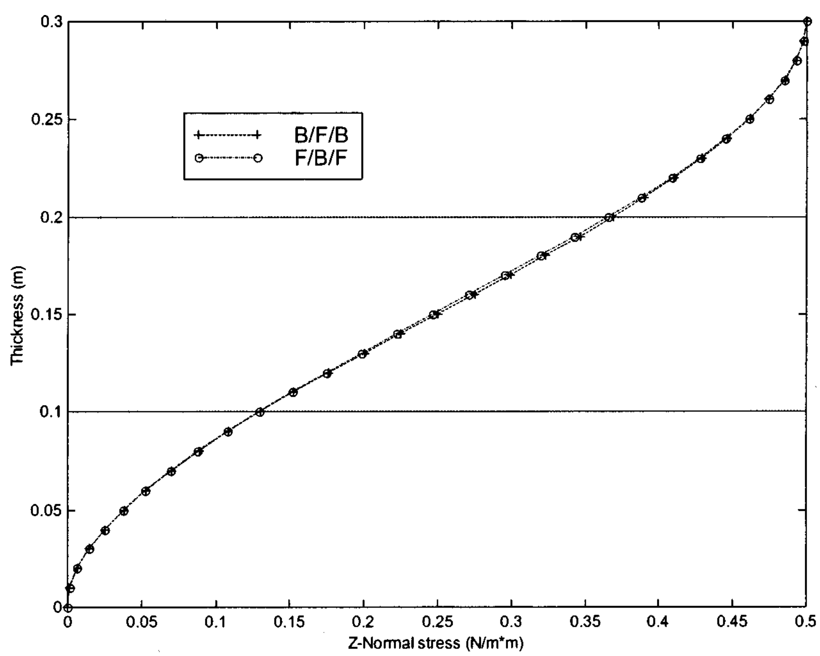

Fig. 10 Variation of the normal stress σ_{zz} along the thickness direction in the sandwich piezoelectric/piezomagnetic plate caused by a surface load on the top surface.

and F/B/F cases are completely different, demonstrating clearly the role played by the material stacking sequences. Furthermore, the slopes of these quantities can be discontinuous across the interface, even though the potentials themselves are continuous.

While Figs. 6 and 7 show the electric displacements D_x ($=D_y$) and D_z, the magnetic displacements (magnetic induction) $B_x(=B_y)$ and B_z are plotted in Figs. 8 and 9. The following general features are observed from these figures:

1 The horizontal electric and magnetic displacements are discontinuous across the interfaces (Figs. 6 and 8).

2 The magnitude of horizontal electric (magnetic) displacement is very small in magnetostrictive $CoFe_2O_4$ (piezoelectric $BaTiO_3$) layer (Figs. 6 and 8). This is due to the fact that for the magnetostrictive $CoFe_2O_4$ (piezoelectric $BaTiO_3$) material, the piezoelectric e_{ij} (piezomagnetic q_{ij}) coefficients are zero.

3 Within the outer layers, the horizontal and vertical electric displacements (magnetic inductions) change dramatically for the B/F/B (F/B/F) case (Figs. 6–9).

4 For these dramatically changed physical quantities, the vertical components reach their maximum magnitudes in the middle of the outer layers (Figs. 7 and 9), while for the horizontal components, the maximums are on the top and bottom surfaces and the minima at the interfaces.

While the electric and magnetic quantities have been greatly influenced by the stacking sequences, relatively small differences have been observed for the corresponding elastic displacements and stresses for these two sandwich cases. For instance, Fig. 10 shows the variation of the normal stress σ_{zz} along the thickness direction in the sandwich piezoelectric/piezomagnetic plates. It is apparent that both stacking sequences produce nearly the same stress distribution, even though the elastic constants for the two materials are considerably different (Tables 1 and 2). This is obviously a coupling phenomenon and can only be explained by resorting to the coupled constitutive relation (1). For the stress field, it is seen from Eq. (1) that it consists of three parts: the elastic constant and strain, the piezoelectric coefficient and electric field, and the piezomagnetic coefficient and magnetic field. Even though the first part may produce quite different stresses in both sandwich plates, the effect of the second and third parts (i.e., the piezoelectric and piezomagnetic terms) is to wipe out, in the present case, the difference of the stress field produced by the first part.

The model results may have potential applications in the field of smart/intelligent structures. For example, to design a sandwich plate made of the magnetostrictive $CoFe_2O_4$ and piezoelectric $BaTiO_3$ materials that requires a given stress level (or distribution) within the plate under a normal surface loading on the top, then in order to produce a large horizontal electric displacement (D_x or D_y) on both the top and bottom surfaces (Fig. 6), the B/F/B stacking sequence should be selected. On the other hand, if a large horizontal magnetic induction (B_x or B_y) on both the top and bottom surfaces (Fig. 8) is expected, then the F/B/F stacking sequence is the choice.

Conclusions

In this paper, we have derived exact solutions for three-dimensional, anisotropic magneto-electro-elastic, simply-supported, and multilayered rectangular plates under both surface and internal loads. We have developed a new and simple formalism that resembles the Stroh formalism so that the homogeneous solution can be obtained in a simple and elegant form. We have also introduced the propagator matrix method in order to treat efficiently and accurately the multilayered case. Our solutions include all the previous solutions, such as the piezoelectric, piezomagnetic, purely elastic solutions, as special cases, and can provide benchmarks for various thick plate theories and numerical methods, such as the finite and boundary element methods.

Two typical numerical examples presented have also shown some significant and interesting features. For instance, responses to an internal load are quite different from those to a surface load, even for a relatively thin plate. The solution to the internal load and its comparison to the corresponding surface loading solution have never been reported in the literature. For sandwich plates made of the piezoelectric $BaTiO_3$ and magnetostrictive $CoFe_2O_4$, we have observed that the stacking sequences (B/F/B and F/B/F) have a clear influence on most physical quantities, in particular, on the electric and magnetic quantities. These features should be of special interest to the design of magneto-electro-elastic composite laminates.

Acknowledgments

The author would like to thank Prof. Paul Heyliger of Colorado State University for his valuable discussions and to the reviewers for their constructive suggestions.

References

[1] Ochoa, O. O., and Reddy, J. N., 1992, *Finite Element Analysis of Composite Laminates*, Kluwer, Boston, MA.
[2] Pagano, N. J., 1969, ''Exact Solutions for Composites in Cylindrical Bending,'' J. Compos. Mater., **3**, pp. 398–411.
[3] Pagano, N. J., 1970, ''Exact Solutions for Rectangular Bidirectional Composites and Sandwich Plates,'' J. Compos. Mater., **4**, pp. 20–34.
[4] Srinivas, S., Rao, C. V. J., and Rao, A. K., 1969, ''Flexure of Simply Supported Thick Homogeneous and Laminated Rectangular Plates,'' Z. Angew. Math. Mech., **49**, pp. 449–458.
[5] Srinivas, S., and Rao, A. K., 1970, ''Bending, Vibration and Buckling of Simply Supported Thick Orthotropic Rectangular Plates and Laminates,'' Int. J. Solids Struct., **6**, pp. 1463–1481.
[6] Pan, E., 1991, ''An Exact Solution for Transversely Isotropic, Simply Supported and Layered Rectangular Plates,'' J. Elast., **25**, pp. 101–116.
[7] Gilbert, F., and Backus, G., 1966, ''Propagator Matrices in Elastic Wave and Vibration Problems,'' Geophysics, **31**, pp. 326–332.
[8] Noor, A. K., and Burton, W. S., 1990, ''Three-Dimensional Solutions for Antisymmetrically Laminated Anisotropic Plates,'' ASME J. Appl. Mech., **57**, pp. 182–188.
[9] Ray, M. C., Rao, K. M., and Samanta, B., 1992, ''Exact Analysis of Coupled Electroelastic Behavior of a Piezoelectric Plate under Cylindrical Bending,'' Comput. Struct., **45**, pp. 667–677.
[10] Ray, M. C., Bhattacharya, R., and Samanta, B., 1993, ''Exact Solutions for Static Analysis of Intelligent Structures,'' AIAA J., **31**, pp. 1684–1691.
[11] Heyliger, P., and Brooks, S., 1996, ''Exact Solutions for Laminated Piezoelectric Plates in Cylindrical Bending,'' ASME J. Appl. Mech., **63**, pp. 903–910.
[12] Heyliger, P., 1997, ''Exact Solutions for Simply Supported Laminated Piezoelectric Plates,'' ASME J. Appl. Mech., **64**, pp. 299–306.
[13] Bisegna, P., and Maceri, F., 1996, ''An Exact Three-Dimensional Solution for Simply Supported Rectangular Piezoelectric Plates,'' ASME J. Appl. Mech., **63**, pp. 628–638.
[14] Lee, J. S., and Jiang, L. Z., 1996, ''Exact Electroelastic Analysis of Piezoelectric Laminae via State Space Approach,'' Int. J. Solids Struct., **33**, pp. 977–990.
[15] Vel, S. S., and Batra, R. C., 2000, ''Three-Dimensional Analytical Solution for Hybrid Multilayered Piezoelectric Plates,'' ASME J. Appl. Mech., **67**, pp. 558–567.
[16] Berlincourt, D. A., Curran, D. R., and Jaffe, H., 1964, ''Piezoelectric and Piezomagnetic Materials and Their Function in Transducers,'' Phys. Acoust., **1**, pp. 169–270.
[17] Landau, L. D., and Lifshitz, E. M., 1984, *Electrodynamics of Continuous Media*, 2nd Ed., Rev. and Enlarged by E. M. Lifshitz and L. P. Pitaevskii, Pergamon Press, New York.
[18] Avellaneda, M., and Harshe, G., 1994, ''Magnetoelectric Effect in Piezoelectric/Magnetostrictive Multiplayer (2-2) Composites,'' J. Intell. Mater. Syst. Struct., **5**, pp. 501–513.
[19] Harshe, G., Dougherty, J. P., and Newnham, R. E., 1993, ''Theoretical Modeling of Multilayer Magnetoelectric Composites,'' Int. J. Appl. Electromagn. Mater., **4**, pp. 145–159.
[20] Nan, C. W., 1994, ''Magnetoelectric Effect in Composites of Piezoelectric and Piezomagnetic Phases,'' Phys. Rev. B, **B50**, pp. 6082–6088.
[21] Benveniste, Y., 1995, ''Magnetoelectric Effect in Fibrous Composites With Piezoelectric and Piezomagnetic Phases,'' Phys. Rev. B, **B51**, pp. 16424–16427.
[22] Huang, J. H., 1998, ''Analytical Predictions for the Magneto-Electric Coupling in Piezomagnetic Materials Reinforced by Piezoelectric Ellipsoidal Inclusions,'' Phys. Rev. B, **B58**, pp. 12–15.
[23] Li, J., and Dunn, M. L., 1998, ''Anisotropic Coupled-Field Inclusion and Inhomogeneity Problems,'' Philos. Mag. A, **A77**, pp. 1341–1350.
[24] Li, J., and Dunn, M. L., 1998, ''Micromachanics of Magnetoelectroelastic Composite Materials: Average Fields and Effective Behavior,'' J. Intell. Mater. Syst. Struct., **9**, pp. 404–416.

[25] Stroh, A. N., 1958, ''Dislocations and Cracks in Anisotropic Elasticity,'' Philos. Mag., **3**, pp. 625–646.
[26] Ting, T. C. T., 1996, *Anisotropic Elasticity*, Oxford University Press, Oxford, UK.
[27] Ting, T. C. T., 2000, ''Recent Developments in Anisotropic Elasticity,'' Int. J. Solids Struct., **37**, pp. 401–409.
[28] Pan, E., 1997, ''A General Boundary Element Analysis of 2-D Linear Elastic Fracture Mechanics,'' Int. J. Fract., **88**, pp. 41–59.
[29] Kausel, E., and Roesset, J. M., 1981, ''Stiffness Matrices for Layered Soils,'' Bull. Seismol. Soc. Am., **71**, pp. 1743–1761.
[30] Datta, S. K., 2000, ''Wave Propagation in Composite Plates and Shells,'' *Comprehensive Composite Materials*, Vol. 1, A. Kelly and C. Zweben, eds., Elsevier, New York, pp. 511–558.
[31] Pan, E., 1997, ''Static Green's Functions in Multilayered Half Spaces,'' Appl. Math. Modelling, **21**, pp. 509–521.
[32] Pan, E., and Datta, S. K., 1999, ''Ultrasonic Waves in Multilayered Superconducting Plates,'' J. Appl. Phys., **86**, pp. 543–551.
[33] Timoshenko, S., and Woinowsky-Krieger, S., 1987, *Theory of Plates and Shells*, McGraw-Hill, New York.
[34] Smittakorn, W., and Heyliger, P. R., 2000, ''A Discrete-Layer Model of Laminated Hygrothermopiezoelectric Plates,'' Mechanics of Composite Materials and Structures, **7**, pp. 79–104.
[35] Huang, J. H., and Kuo, W. S., 1997, ''The Analysis of Piezoelectric/Piezomagnetic Composite Materials Containing Ellipsoidal Inclusions,'' J. Appl. Phys., **81**, pp. 1378–1386.